AWARD NUMBER: W81XWH-13-1-0481

TITLE: Quantitative, Noninvasive Imaging of DNA Damage in Vivo of Prostate Cancer Therapy by Transurethral Photoacoustic (TUPA) Imaging

PRINCIPAL INVESTIGATOR: Liangzhong Xiang

CONTRACTING ORGANIZATION: The Leland Stanford Junior University
Stanford, CA 94305

REPORT DATE: October 2014

TYPE OF REPORT: Annual

PREPARED FOR: U.S. Army Medical Research and Materiel Command
Fort Detrick, Maryland 21702-5012

REPORT DOCUMENTATION PAGE

Form Approved
OMB No. 0704-0188

1. REPORT DATE	2. REPORT TYPE	3. DATES COVERED
October 2014	Annual	30 SEP 2013 -29 SEP 2014

4. TITLE AND SUBTITLE

Quantitative, Noninvasive Imaging of DNA Damage *in Vivo* of Prostate Cancer Therapy by Transurethral Photoacoustic Imaging

5a. CONTRACT NUMBER

5b. GRANT NUMBER
W81XWH-13-1-0481

5c. PROGRAM ELEMENT NUMBER

6. AUTHOR(S)

Liangzhong Xiang

E-Mail: xianglzh@stanford.edu

5d. PROJECT NUMBER

5e. TASK NUMBER

5f. WORK UNIT NUMBER

7. PERFORMING ORGANIZATION NAME(S) AND ADDRESS(ES)

The Leland Stanford Junior University
Stanford, CA 94305

8. PERFORMING ORGANIZATION REPORT NUMBER

9. SPONSORING / MONITORING AGENCY NAME(S) AND ADDRESS(ES)

U.S. Army Medical Research and Materiel Command
Fort Detrick, Maryland 21702-5012

10. SPONSOR/MONITOR'S ACRONYM(S)

11. SPONSOR/MONITOR'S REPORT NUMBER(S)

12. DISTRIBUTION / AVAILABILITY STATEMENT

Approved for Public Release; Distribution Unlimited

13. SUPPLEMENTARY NOTES

14. ABSTRACT

The first year of this research program developed the foundation for a new medical imaging modality, now called Trans-Urethral Photoacoustic (TUPA) Imaging, which utilizing a small catheter into the urethra enabling imaging molecular marker of DNA Damage during prostate radiation therapy with high photoacoustic contrast and resolution. The development of this modality is significant to the tracking the biologic effect of radiation treatment, rather than just the physical dose. The work in Year 1 developed the imaging instrumentation to enable this modality. This grant has provided the funding to devise a trans-urethral photoacoustic endoscope, which has the potential to obtain higher resolution by using a high frequency ultrasound detector and achieve deeper penetration depth with a light delivery via the urethra. As part of the first-year training goals, this grant has provided the opportunity for extensive training in prostate cancer, molecular targeting of cancer, molecular imaging modalities, and opportunities to engage physicians to design appropriate tools. As of today, the results of this grant are: 2 journal publications, 4 conference abstracts, including 3 first author, and 2 conference oral presentations. The future for this grant looks bright, as this technique will soon be tested in small animal models *in vivo*; the next, more clinically feasible interventional version is under development.

15. SUBJECT TERMS

PROSTATE CANCER, PHOTOACOUSTIC IMAGING, MOLECULAR IMAGING, RADIATION THERAPY

16. SECURITY CLASSIFICATION OF:			17. LIMITATION OF ABSTRACT	18. NUMBER OF PAGES	19a. NAME OF RESPONSIBLE PERSON
a. REPORT	b. ABSTRACT	c. THIS PAGE			USAMRMC
Unclassified	Unclassified	Unclassified	Unclassified	16	19b. TELEPHONE NUMBER *(include area code)*

Table of Contents

Page

1. INTRODUCTION

The goals of the first year of this training grant were to develop the foundations for a new medical imaging modality, now called Trans-Urethral Photoacoustic (TUPA) Imaging, which utilizing a small catheter into the urethra enabling imaging molecular marker of DNA Damage during prostate radiation therapy with high photoacoustic contrast and resolution. The development of this modality is significant to tracking the biologic effect of radiation treatment, rather than just the physical dose[1-6].

The first-year research goals were to develop the imaging instrumentation to enable this modality. This grant has provided the funding to devise a trans-urethral photoacoustic endoscope, which has the potential to obtain higher resolution by using a high frequency ultrasound detector and achieve deeper penetration depth with a light delivery via the urethra. For the first-year training goals, this grant has provided for extensive study in prostate cancer, molecular imaging modalities, molecular targeting of cancer, and opportunities to engage physicians.

As of today, the results of this grant are: **2** journal publications; **4** conference abstracts, including **3** first author, and **2** conference oral presentations. The future for this grant looks bright, as this technique will soon be tested in small animal models *in vivo*; the next, more clinically feasible interventional version is under development.

2. KEYWORDS

Prostate Cancer, Photoacoustic Imaging, Molecular Imaging, Radiation Therapy

3. OVERALL PROJECT SUMMARY

Research Accomplishments: SOW Aim 1: Develop a photoacoustic imaging system for prostate cancer imaging

Major Task 1: Develop photoacoustic imaging system

Subtask 1: Investigation of photoacoustic imaging system (month 1-6)

The trans-urethral photoacoustic (TUPA) catheter has been developed in the first 6 month of this project, shown in Figure 1. Figure 1(a) is a schematic to illustrate the principle of the mechanical scanning and the configuration of the optical and acoustic components. The catheter was built with a side-fire optical fiber for light delivery and a commercially available mini ultrasound transducer. The catheter was capable of both receiving the photoacoustic signal and performing ultrasound pulse-echo imaging[8].

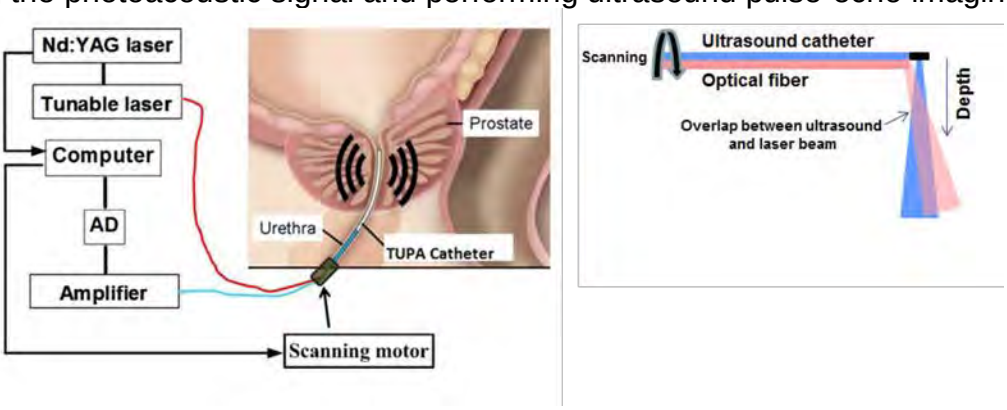

Figure 1 (a) Schematic of trans-urethral photoacoustic (TUPA) system

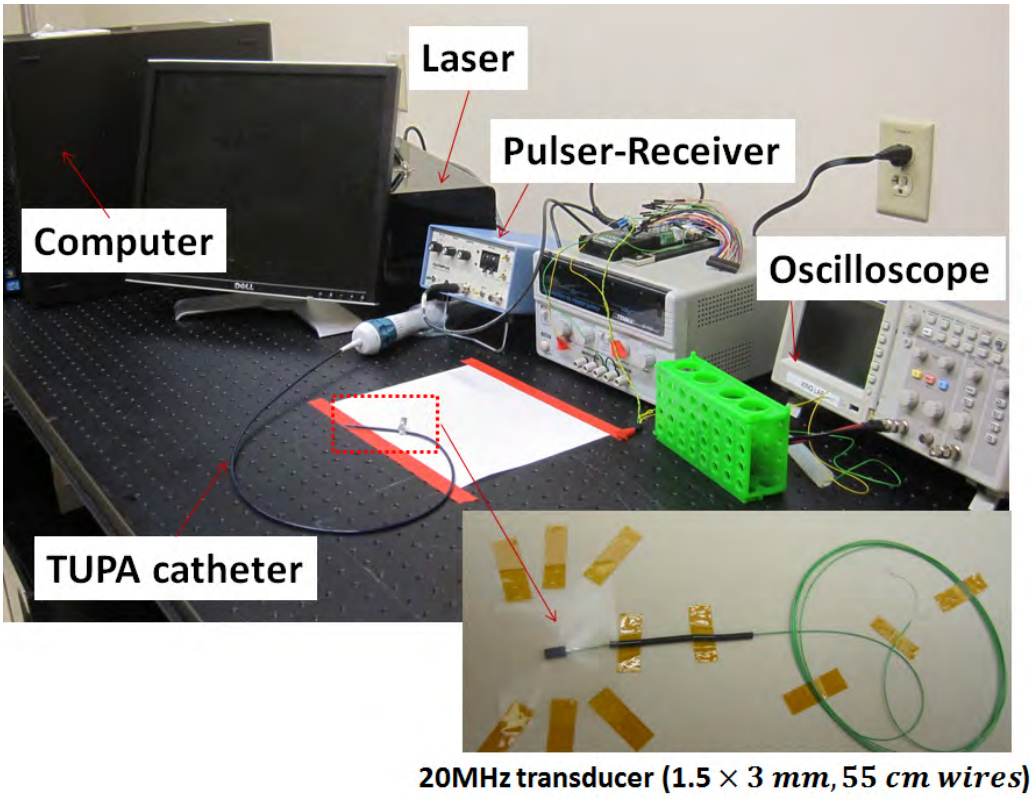

Figure 1 (b) Picture of the trans-urethral photoacoustic (TUPA) system and its key components

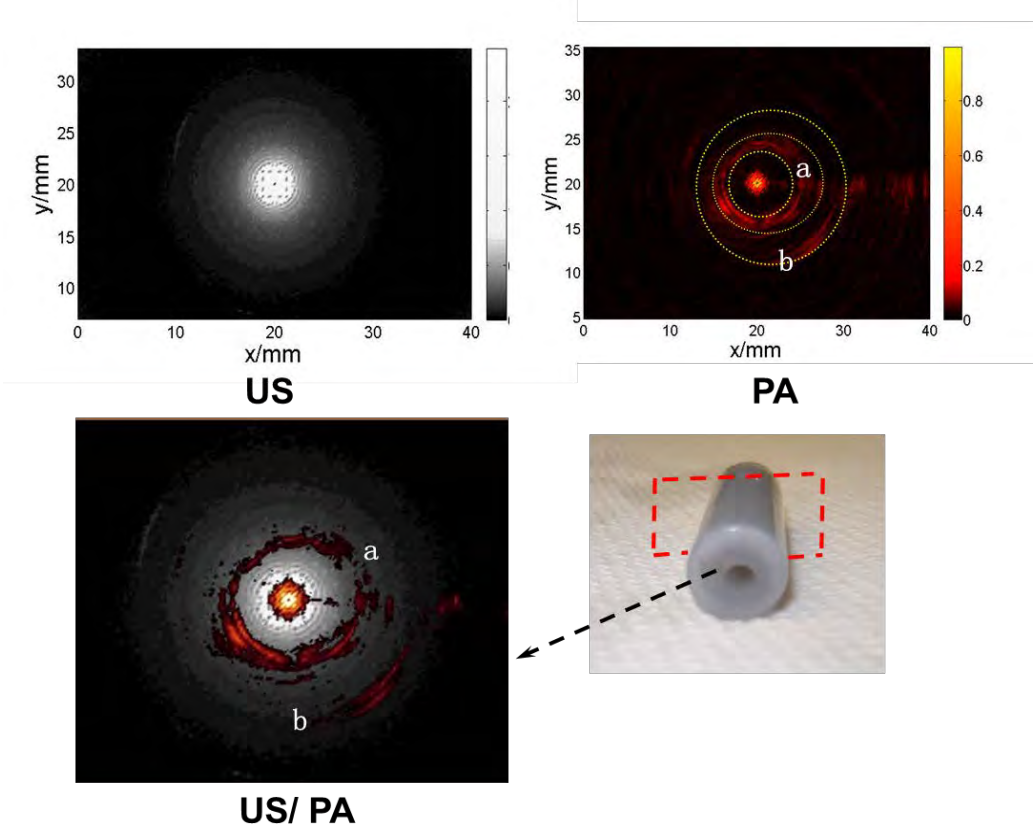

Figure 1 (c) Phantom experiments by using trans-urethral photoacoustic (TUPA) system. US : ultrasound imaging of the phantom; PA: Photoacoustic imaging of the phantom; and combined US/PA imaging of the phantom; and the picture of the phantom.

Figure 1(b) shows photos of trans-urethral photoacoustic (TUPA) imaging system. A TUPA catheter comprised of two key components: optical laser fiber, and the mini ultrasound transducer. An ultrasonic (US) transducer (LiNbO3, ~20 MHz, unfocused) generates US pulses and detects both PA and US pulse-echo signals. The US transducer was costumed made by Blatek, Inc. with a very small piezoelement size (1.5x3 mm). It provides two 55cm wires which can send the photoacoustic signal outside of the catheter to the ultrasound pulser and receiver (5072PR, Olympus). Inside the tubular shaft, a multimode optical fiber (UM22-600, Thorlabs) was placed which is positioned statically along the axis of the endoscope. A parabolic acoustic reflector (10 mm diameter, nickel substrate, Optiforms) and an optical prism (3 mm diameter, altered from #45-525, Edmund) was mounted inside the catheter. The scanning head is actuated by a step motor located at the proximal end. Via the prism and parabolic reflector, laser pulses and acoustic waves are delivered coaxially to achieve an efficient overlap of the illumination and acoustic detection over a large depth range. A membrane forms an imaging window and seals the inner cavity of the endoscope, which is filled with de-ionized water. The imaging capability of combined PA and US imaging with endoscopic catheter has been demonstrated on a phantom imbedded with IRDye 800CW as a contrast agent in the sample (Figure 1(c)).

This work was carried out under guidance from my mentor Dr. Lei Xing, as proposed, who is an expert in medical imaging instrumentation.

Subtask 2: Control software will be developed in Labview to enable automated data acquisition (month 7-12)

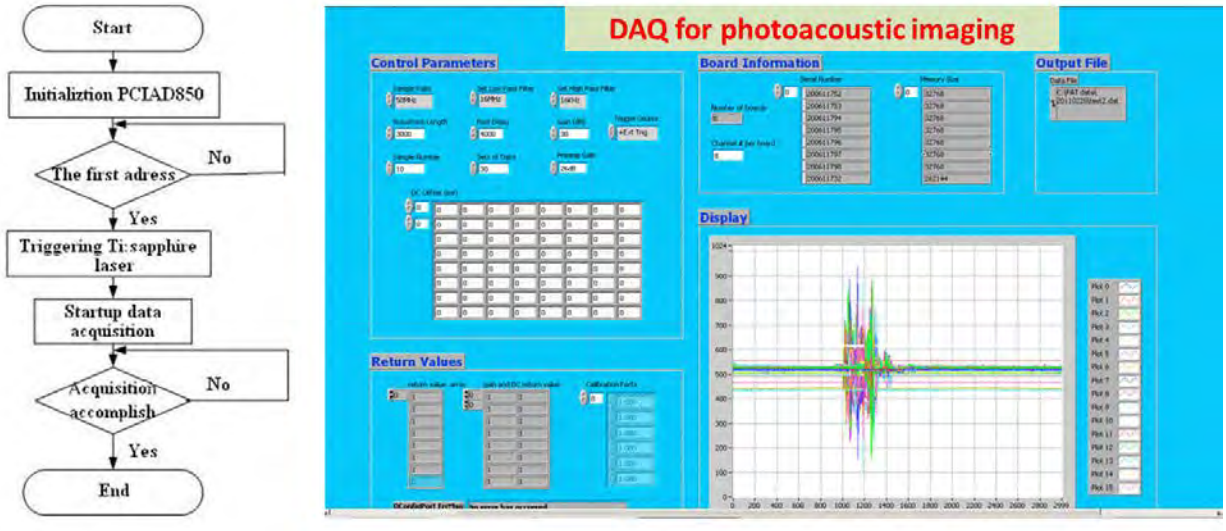

Figure 2 Flowchart of the photoacoustic data acquisition loop, and control panel of data acquisition software for photoacoustic imaging

A Labview based platform was built to control the data acquisition system (Figure 2). The 2-D PA/US image was reconstructed with the modified filtered back projection algorithm constructed in the MATLAB programming language. Light and ultrasound attenuation was considered during the imaging reconstruction. Image registration between PA and

US has been done automatically in the software. The reconstructed data from a pullback scan can then be used to generate a 3-D PA/US image.

Training Accomplishments:

Major Task 1: Training and educational development in prostate cancer research

Subtask 1: Attend radiation physics resident lecture series *(month 1-6)*

Stanford University Radiation Oncology has a comprehensive training program that emphasizes on research with ambitious clinical goals. I attended weekly research seminars (every Tuesday morning) held by the department, where Stanford faculty members, postdoctoral fellows, as well as invited speakers from outside give presentations and open discussions on their research. Some of the seminars are very impressive to me. For example, one of the seminars tittled as "Image Guidance in Radiation Therapy: Applications to Adaptive Treatment Planning and Response" is really help me understand the current clinical needs in radiation therapy. In addition, to keep up with the fast development of radiation physics research, I also attended biweekly radiation physics journal club meetings to discuss and exchange ideas about the most recent research. The comprehensive training program and an easily accessible talent pool at Stanford have contributed significantly to the success of the proposed research.

Subtask 2: Present research at the monthly department group meetings *(month 1-24)*

It is required to present my research at the monthly department group meetings here at Stanford. My mentor Dr. Lei Xing and other members have been invited. In those group meetings, we discussed the progress of current projects and the latest progresses in prostate cancer research, molecular imaging, bioengineering, or related fields. After each presentation, the advisory team provided constructive feedback and advice on his research and presentation skills. I was also invited to present my research at the Stanford Radiation Biology Seminar on August 12th, 2014 titled as "Radiation induced acoustic emission for cancer imaging and diagnosis".

Subtask 3: Attend a national scientific meeting in relevant scientific field *(month 1-24)*

I attended the annual meetings held by professional societies in the field, such as American Society of Therapeutic Radiology and Oncology (ASTRO) on 09/15/2014 at San Francisco, California, and American Association of Physicists in Medicine (AAPM) on 07/22/2014 at Texas Austin, etc. These scientific meetings offer an ideal platform for me to communicate and exchange ideas about the latest development related to the proposed research with peers around the globe.

In performing these tasks, the investigator has been exposed to the field of molecular imaging, a new direction for this PI. This research education has been aided with participation in BioE222: Molecular Imaging, which brought together the top molecular imaging faculty at Stanford to teach aspects in the hardware, chemistry, and biology of molecular imaging. In addition, the PI was exposed to molecular probe fabrication, including the processes in making IRDye stable in human serum with low toxicity.

Also, the PI gained knowledge in molecular targets, and the advantages and disadvantages of targeting to peptides, hormones, antibidies, affabodies, and other targeting agents. This program has been aided by working at benchside with these materials scientists, biologists, and molecular imaging experts.

4. KEY RESEARCH ACCOMPLISHMENTS

- Developed a trans-urethral photoacoustic (TUPA) imaging, in an appropriate geometry for monitoring of Radiation Therapy for prostate cancer patient.
- Fabricated a trans-urethral photoacoustic (TUPA) imaging catheter to enable automated, controlled imaging of the DNA damage during prostate cancer radiation therapy.
- A Labview based software platform was built to control the data acquisition system for photoacoustic imaging.

5. CONCLUSION

The first funding period in this grant has developed the research infrastructure for trans-urethral photoacoustic (TUPA) imaging. This has resulted in a fully functioning system that may perform the systematic studies in phantoms and pre-clinical animals that is the crux of Aims 3 & 4 from the SOW. Towards the goal of determining the feasibility for patient imaging, and we will provide proof-of-concept for the prostate cancer treatment monitoring realizations of this modality. Future work for Aims 3&4 will involve a more sophisticated tissue-simulating phantom study to evaluate system temporal and sensitivity performance with regards to imperfect background contrast uptake, and a systematic study to determine the feasibility in pre-clinical and clinical research. In addition, the first funding period for this grant resulted in much training for the PI, for molecular imaging, small-animal imaging, cancer biology, and device commercialization. The research and training in the grant are significant for the eradication of prostate cancer for the new developments in the potential for early detection of prostate cancer, for the treatment of prostate cancer by providing feedback to guide radiation therapy, and for the coursework which will enable this PI to apply newly learned skills to bring technologies to the clinic and marketplace. It is our hope that this pioneering work will lead to advancements in this new field that can be translated to the clinic.

6. PUBLICATIONS, ABSTRACTS, AND PRESENTATIONS

2 journal publications, 1 patent application; 4 conference abstracts, including 3 first author, and 2 conference oral presentations; 4 courses taken, including BioE222: Molecular Imaging, Med374: Medical Device Design. The future for this grant looks bright, as this technique will soon be tested in small animal models *in vivo*; the next, more clinically feasible interventional version is under development.

Presentations:

- **Liangzhong Xiang**, Benjamin P Fahimian, Moiz Ahmad, and Lei Xing, "High precision focal brachytherapy of prostate cancer guided by dual-model photoacoustic and ultrasound imaging" Presented at 56th Annual Meeting, San Francisco, California, on 09/13/2014. Poster
- **L Xiang**, M Ahmad, A Nikoozadeh, G Pratx, B Khuri-Yakub, L Xing, "X-ray acoustic computed tomography (XACT): 100% sensitivity to X-ray absorption", Presented at 56th Annual Meeting&. Exhibition, Austin, Texas, on 07/22/2014. Oral Presentation
- **Liangzhong Xiang**, M Ahmad, C Carpenter, G Pratx, A Nikoozadeh, B Khuri-Yakub, L Xing, "X-Ray Acoustic Computed Tomography: Concept and Design", Presented at 55th Annual Meeting&. Exhibition, Indianapolis, Indiana, on 08/08/2013. Hot Topic Oral Presentation
- M Ahmad, M Bazalova, **L Xiang**, L Xing, "X-Ray Fluorescence CT as a Novel Imaging Modality for Improved Radiation Therapy Target Delineation", Presented at 56th Annual Meeting, San Francisco, California, on 09/13/2014. Poster

Journal Publications:

- **Liangzhong Xiang**, Moiz Ahmad, Xiang Hu, Zhen Cheng, and Lei Xing, Label-free photoacoustic cell-tracking in real-time, *X-Acoustics: Imaging and Sensing*, 1: 18-22 (2014).
- Moiz Ahmad, Magdalena Bazalova, **Liangzhong Xiang**, and Lei Xing, Order of magnitude sensitivity increase in x-ray fluorescence computed tomography (XFCT) imaging with an optimized spectro-spatial detector configuration: theory and simulation, *IEEE Trans. Med. Imag.*, 99, (2014).

7. INVENTIONS, PATENTS AND LICENSES

- **Liangzhong Xiang**, Lei Xing, "Method, system and apparatus for ionizing radiation-induced acoustic tomography," US Patent Application (Pending, 2013).

8. REPORTABLE OUTCOMES

2 journal publications, 1 patent application;4 conference abstracts, including 3 first author, and 2 conference oral presentations; 4 courses taken, including BioE222: Molecular Imaging, Med374: Medical Device Design. The future for this grant looks bright, as this technique will soon be tested in small animal models *in vivo*; the next, more clinically feasible interventional version is under development.

9. OTHER ACHIEVEMENTS

Nothing to report.

10. REFERENCES

1. Evaluation of the efficacy of radiation-modifying compounds using gH2AX as a molecular marker of DNA double-strand breaks, Genome Integrity 2(3)(2011):1-11.
2. Sedelnikova OA, Pilch DR, Redon C, Bonner, WM: Histone H2AX in DNA damage and repair. Cancer Biology & Therapy, 2(2003):233-235.
3. Wenrong Li, Fang Li, Qian Huang, Quantitative, Noninvasive imaging of radiation-induced DNA, Cancer Res; 71(12) (2011): 4130.
4. Qvarnstrom OF, Simonsson M, Johansson KA, Nyman J, Turesson I. DNA double strand break quantification in skin biopsies. Radiother Oncol., 72(2004):311–7.
5. Olive PL. Detection of DNA damage in individual cells by analysis of histone H2AX phosphorylation. Methods Cell Biol. 75(2004): 355–73.
6. Bart Cornelissen, Veerle Kersemans, Sonali Darbar, James Thompson, Ketan Shah, Kate Sleeth, Mark A. Hill, and Katherine A. Vallis, Imaging DNA damage in vivo using γH2AX-targeted immunoconjugates, Cancer Res. 71(13)(2011): 4539–4549.Liangzhong Xiang, Benjamin P Fahimian, Moiz Ahmad, and Lei Xing, “High precision focal brachytherapy of prostate cancer guided by dual-model photoacoustic and ultrasound imaging” Presented at 56th Annual Meeting, San Francisco, California, on 09/13/2014
7. Liangzhong Xiang, Moiz Ahmad, Xiang Hu, Zhen Cheng, and Lei Xing, Label-free photoacoustic cell-tracking in real-time, *X-Acoustics: Imaging and Sensing*, 1: 18-22 (2014).
8. Liangzhong. Xiang, Benjamin P Fahimian, Moiz Ahmad, Mark Buyyounouski, James Brooks, Lei. Xing, Photoacoustic and ultrasound image-guided focal brachytherapy of prostate cancer, in preparation, (2014).

11. APPENDIX

individually for statistical purposes. All treatments completed with 6 MV photons at 200cGy per treatment (linear accelerator).

Results: The dose contributions from each of the 5 treatments without and with the prone lead shield to the medial (MCB) and lateral (LCB) contralateral breast were averaged individually. Unshielded dose means were 36.2cGy and 3.47cGy ($p = 1.53x10\text{-}10$), and shielded dose means were 10.08cGy and 1.57cGy ($p = 1.21x10\text{-}8$), respectively. When comparing MCB and LCB doses without and with lead, the shield significantly reduced dose to both sides of the contralateral breast (MCB $p = 4.34x10\text{-}11$, LCB $p = 9.96x10\text{-}4$).

Conclusions: The prone lead shield significantly reduced scatter dose to the contralateral breast. Reductions may be clinically relevant by decreasing the risk of contralateral radiation-induced breast cancer in patients receiving radiation therapy for breast cancer. This shield is safe and would not require adjustment as it would be a part of the prone breast board during treatments.

Author Disclosure: **U. Goyal:** None. **G. Georgiev:** None. **M. Ceizyk:** None. **A. Locke:** None. **H. Thai:** None. **C. Hine:** None. **K. Bowers:** None. **A. Mignault:** None. **L. Castillo:** None. **L. Smith-Raymond:** None.

3849

High Precision Focal Brachytherapy of Prostate Cancer Guided by Dual-Mode Photoacoustic and Ultrasound Imaging

L. Xiang, B.P. Fahimian, M. Ahmad, M. Buyyounouski, and L. Xing; *Stanford University, Palo Alto, CA*

Purpose/Objective(s): Prostate focal brachytherapy can potentially be leveraged for ablative dose escalation of biologically targeted lesions and for eligible early stage patients, as a sole treatment method to reduce normal tissue toxicity relative whole-gland brachytherapy. However, its current implementation is limited by the lack of an imaging technique that can precisely localize and stage the tumor, and provide real-time feedback of the seed implantation with high resolution. The purpose of this study is to explore a new dual-mode photoacoustic (PA) and ultrasound (US) imaging technique to address these needs.

Materials/Methods: Phantom experiments were performed to simulate PA/US imaging of a brachytherapy seed implantation. A dual-modality PA/US imaging system was engineered. This system consisted of: 1) A tunable OPO laser beam pumped by a pulsed Nd:YAG laser (wavelength from 690−960 nm) delivered through an optical fiber bundle to generate PA signal; and 2) an array transducer (13-24 MHz) to acquire both PA and US signals. Once the photoacoustic transient and ultrasound pulse-echo signal was captured, the image processing was performed with the acquired imaging data. The phantom consisted of lipid emulsion solution (Intralipid) to mimic tissue scattering, and Agar powder (2%) to solidify the mixed Intralipid and India ink to simulate tissue absorption. A hypodermic needle and titanium-shelled 4.5 x0.8-mm brachytherapy seeds were used for the implantation experiment.

Results: The needle was imaged with excellent PA contrast (11.5±5 ratio between the needle and the background tissue at a laser wavelength of 750 nm) with insertion captured in real-time. We have found that photoacoustic imaging at 850 nm can identify brachytherapy seeds uniquely with a contrast-to-noise ratio of 51.6 dB. The co-registered images of PA imaging and US imaging are able to clearly display the presence of the brachytherapy seed within the tissue background.

Conclusions: The PA imaging has been validated that there are high contrast-to-noise ratio in visualizing tumor based on the optical contrast between tumor vasculature and the soft tissue, while US imaging presents the morphological features including the boundary and the urethral of the prostate. In addition to the potential of improving tumor localization accuracy, the proposed combined PA and US imaging approach can allow for the real-time visualization of needle insertion during a prostate seed implantation, and high resolution verification of seed location after implantation. Such a capability would improve adherence to a patient's dosimetric treatment plan, may allow for intraoperative dynamic dose optimization, and could obviate the need for costly, ionizing CT-based post-implant evaluations and external-beam radiation corrections.

Author Disclosure: **L. Xiang:** None. **B.P. Fahimian:** None. **M. Ahmad:** None. **M. Buyyounouski:** None. **L. Xing:** None.

3850

The Credentialing Process for the NSABP B-51/RTOG 1304 Phase 3 Randomized Clinical Trial

J. Leif,[1] H. Nguyen,[1] A. Hollan,[1] D. Followill,[1] J. Galvin,[2,3] D. Kiniry,[4,5] T.B. Julian,[5,6] E.P. Mamounas,[5,7] J. White,[3,8] A.J. Kahn,[5,9] S. Shaitelman,[3,1] M. Torres,[3,10] F. Vicini,[5,11] N. Wolmark,[5,12] and W.J. Curran[3,10]; *[1]U.T. M.D. Anderson Cancer Center, Houston, TX, [2]Thomas Jefferson University Hospital, Philadelphia, PA, [3]Radiation Therapy Oncology Group (RTOG), Philadelphia, PA, [4]NSABP Biostatistical Center and the University of Pittsburgh Graduate School of Public Health, Department of Biostatistics, Pittsburgh, PA, [5]National Surgical Adjuvant Breast and Bowel Project (NSABP), Pittsburgh, PA, [6]Allegheny Cancer Center at Allegheny General Hospital, Pittsburgh, PA, [7]M.D. Anderson Orlando, Orlando, FL, [8]Ohio State University, Columbus, OH, [9]The Cancer Institute of New Jersey, Rutgers Cancer Institute of New Jersey, New Brunswick, NJ, [10]Emory University Winship Cancer Institute Emory University, Atlanta, GA, [11]William Beaumont Hospital, Royal Oak, MI, [12]Allegheny Cancer Center at Allegheny, Pittsburgh, PA*

Purpose/Objective(s): NSABP B-51/RTOG 1304 is a randomized phase III clinical trial evaluating regional nodal (RN) radiation therapy (RT) in patients (pts) with positive axillary nodes before neoadjuvant chemotherapy (NC) who convert to negative axillary nodes (ypN0) after NC. Pts following lumpectomy are randomized to whole breast RT (Arm 1A) vs breast and RN RT (Arm 2A); and post-mastectomy pts are randomized to observation (Arm 1B) vs chestwall and RN RT (Arm 2B). This is the first multi-institution group trial evaluating breast cancer RN RT, requiring 3DCRT or IMRT treatment plans based on CT contouring with DVH plan evaluation. An institution must be credentialed to demonstrate that physician's staff have read the protocol, meet specific technology requirements, and generate RT plans that meet protocol-defined RT dose volume constraints. The credentialing goal is to reduce protocol deviations and provide institutional feedback to correct unacceptable variations before pt enrollment.

Materials/Methods: Credentialing includes completing a Facility Questionnaire and developing 3DCRT and/or IMRT treatment plan for 3 CT benchmark cases for: Arm 1A - breast RT only; 2A - breast and RN RT; and 2B - post-mastectomy chestwall and RN RT downloaded from the Radiological Physics Center's (RPC) website. RN RT includes dose coverage of supraclavicular, axillary, and internal mammary nodes in the first 3 intercostal spaces. RPC reviews the benchmarks using MIM to verify that the dose to targets and constraints to organs at risk meet protocol-specified criteria. Credentialed intuitions may then enroll pts. The first case enrolled on Arms 2A and 2B undergo pre-treatment review and are scored per protocol: variation acceptable or variation unacceptable.

Results: NSABP B-51/ RTOG 1304 opened 8-22-2013 with a targeted accrual of 1,601. 101 institutions have initiated the credentialing process. 94 that have submitted benchmarks for review with 7% failed and never resubmitted. Credentialed techniques are 4% IMRT only, 52% 3DCRT only, and 44% 3DCRT and IMRT. Benchmark initial failure rates requiring re-submission are: 6% failed the benchmark for breast RT only (1A); 11% failed 2B post-mastectomy chestwall and RN RT; and 40% failed 2A breast and RN RT at least once before being credentialed. 9% of the institutions failed 2A twice and 1 failed three times. 87 are credentialed to enter pts. 9 enrolled cases have had pre-treatment reviews and 2 scored "unacceptable" with re-submission for re-review due to target volume contouring.

Conclusions: NSABP B-51/ RTOG 1304 credentialing prepares institutions for RT delivery to meet protocol requirements. This revealed Arm 2A, breast RT and RN RT has required resubmission most for institutions to meet protocol guidelines.

Acknowledgment: This research was supported by NCI PHS U10−CA−12027, -69651, -37377, -69974, -2166.

Author Disclosure: **J. Leif:** None. **H. Nguyen:** None. **A. Hollan:** None. **D. Followill:** None. **J. Galvin:** None. **D. Kiniry:** None. **T.B. Julian:** None. **E.P. Mamounas:** None. **J. White:** None. **A.J. Kahn:** None. **S. Shaitelman:** None. **M. Torres:** None. **F. Vicini:** None. **N. Wolmark:** None. **W.J. Curran:** None.

X Acoustics:Imaging and Sensing
Research Article

Open Access

Liangzhong Xiang, Moiz Ahmad, Xiang Hu, Zhen Cheng, and Lei Xing*

Label-free Photoacoustic Cell-Tracking in Real-time

Abstract: Cell-tracking method has an important role in detection of metastatic circulating tumor cells (CTCs) and cell-based therapies. Label-free imaging techniques are desirable for cell-tracking because they enable long time observations without photobleaching in living cells or tissues where labeling is not always possible. Photoacoustic microscopy is a label-free imaging technique that offers rich contrast based on nonfluorescent cellular optical absorption associated with intrinsic chromophores and pigments. We show here that photoacoustic imaging is feasible for detecting very low numbers ($\times 10^4$) of melanoma cells without labeling because of the strong instinct optical absorption of melanin in near-infrared wavelength. Flowing melanoma cells are imaged with micrometer-resolution (40 μm) and penetration depths of centimeters (13 mm) in real-time. Photoacoustic imaging as a new cell-tracking method provides a novel modality for cancer screening and offers insights into the underlying biological process of cancer growth and metastasis and cell therapy.

DOI 10.2478/phto-2014-0002
Received March 15, 2014; accepted April 23, 2014.

1 Introduction

The ability to follow the distribution and migration of cells in living organisms is crucial for both the development of metastatic circulating tumor cells (CTCs) detection and cell-based therapies [1, 2]. Several technologies exist that are able to noninvasively track cells *in vivo*, each with its own advantages and disadvantages in terms of cell tracking performance. MRI is unique in that three-dimensional, high resolution images can be acquired regardless of tissue depth without the use of ionizing radiation [3]. However, the shortcomings of MRI are that it is not sensitive enough to visualize a small number of cells, requires expensive equipment, and offers relatively low imaging speeds. PET and SPECT modalities are more sensitive, but rely on the detection of radioactive decay. The probes and detection methods raise important safety considerations to the patient and potentially interfere with cellular therapy [4]. Optical methods show great promise in small animal experiments; however, the imaging penetration depth is limited by the low tissue penetration of light [1]. Furthermore, optical florescence imaging relies on the use of fluorescent labels or dyes, which may be toxic or perturbative to cells, and are subject to photobleaching. It is therefore difficult to use them for studying long-term biological dynamics within living cells. Non-invasive label-free imaging techniques are desirable because they allow for long time observations in living cells or tissues where labeling is not always possible [5].

Photoacoustic microscopy (PAM) is a label-free imaging technique that offers rich contrast based on optical absorptions of the endogenous chromophores (e.g., hemoglobin or melanin), and provides higher spatial resolution in deeper tissue compared with most optical modalities [6–9]. Historically, label-free PAM has been successfully applied to *in vivo* imaging of hemoglobin and melanin, two major sources of endogenous optical absorption in biological tissue in the visible spectral range. Recently, additional photoacoustic contrast mechanisms have been demonstrated by exciting myoglobin [10] and bilirubin [11] with visible illumination, DNA and RNA in nuclei [12] with ultraviolet (UV) illumination, and water [13] and lipid [14] with near-infrared illumination. In fact, PAM can potentially image any molecule that has sufficient absorption at specific wavelengths without fluorescent label [15]. Unfortunately, long scan times are presently required in high resolution PAM [8, 16].

Liangzhong Xiang, Moiz Ahmad: Department of Radiation Oncology, School of Medicine, Stanford University, Stanford, CA USA 94305 USA
Xiang Hu, Zhen Cheng: Molecular Imaging Program at Stanford (MIPS), Department of Radiology and Bio-X Program, Canary Center at Stanford for Cancer Early Detection, Stanford University, California, 94305-5344 USA
***Corresponding Author: Lei Xing:** Ph.D., DABR, Department of Radiation Oncology, Stanford University, 875 Blake Wilbur Drive Room G233, Stanford, CA 94305-5847, Ph: (650) 498-7896, Fax: (650) 498-4015, E-mail: lei@stanford.edu, http://xinglab.stanford.edu

Here we present a high-frequency (40 MHz central frequency) PAM system capable of dynamically tracking the melanoma cells with high spatial resolution. We show that photoacoustic imaging is feasible for detecting very low numbers ($\times 10^4$) of melanoma cells without labeling. Flowing melanoma cells are imaged with micrometer-resolution (40 μm) and centimeter-penetration depth (13 mm) in real-time.

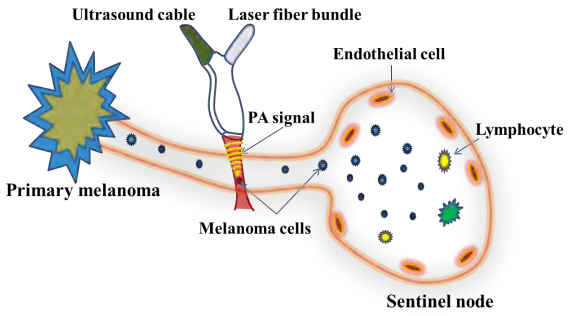

Fig. 1. Schematic of photoacoustic cell-tracking technique.

2 Methods and Materials

2.1 Combined photoacoustic and ultrasound (PA/US) imaging

Photoacoustic and ultrasound images were taken using Visual Sonics Vevo LAZR Photoacoustics Imaging System (*FUJIFILM Visualsonics, Inc.; Toronto, Canada*). A tunable (680-970 nm) OPO laser beam pumped by Nd:YAG laser delivers < 10 ns duration pulses (*OPOTEK Inc., Carlsbad, CA, USA*) through an optical fiber bundle to the phantom with repetition frequency of 20 Hz. The fiber bundle was combined with the ultrasound transducer and aligned such that the transmitted light was focused at the focal point of the transducer. A high frequency linear array transducer centered at 40 MHz ((22- to 55-MHz imaging band) was used to record the photoacoustic signal and pulse-echo ultrasound signal. As Fig. 1 illustrates, when a melanoma cell passes through the laser focal zone, a time sequence of photoacoustic pulses is generated. The trigger signal from the laser system was synchronized with ultrasound imaging system to capture the photoacoustic signal upon laser irradiation. PA and US images were reconstructed from the acquired data. Combined ultrasound and photoacoustic images were created by overlaying photoacoustic intensities higher than a user-defined threshold on the grayscale ultrasound images. The system supports real-time B-mode imaging with spatial resolution down to 40 μm [17].

2.2 Tissue mimicking phantom experiments with melanoma cell inclusions

Accurate quantification of cells with high sensitivity is one of the essential requirements for effective cell tracking methods. Additionally, the ability to track cells at depth in tissue is highly desirable. To evaluate the sensitivity and depth-performance of photoacoustic imaging, an *in vitro* experiment using a tissue mimicking gelatin phantom was performed. The phantom was made with a lipid emulsion solution (Intralipid) to mimic tissue scattering (optical scattering coefficient $\mu'_s = 1.0\ \text{mm}^{-1}$), India ink (optical absorption coefficient $\mu_a = 0.007\ \text{mm}^{-1}$) to simulate tissue absorption and Agar powder (2%) to solidify the mixed Intralipid and India ink [18]. The five inclusions (10 μL each) were composed of gelatin solutions mixed with melanoma cells suspended in cell culture medium at five different concentrations of cells (2.5×10^3 cells/μL, 5×10^3 cells/μL, 1×10^4 cells/μL, 2×10^4 cells/μL and 4×10^4 cells/μL) were embedded in the gel phantom at depth of 10 mm. B16F10 mouse melanoma cells were obtained directly from a cell bank (American Type Culture Collection). Cells were cultured using standard procedures, including serial passage in phenol-free RPMI 1640 (Invitrogen) supplemented with 10% fetal bovine serum (Invitrogen).

3 Results

3.1 Quantification of the cell detection sensitivity

For the cell detection sensitivity experiment, the melanoma B16F10 cells were located at 10 mm underneath the surface of gel phantoms. Figure 2a shows the ultrasound (top), photoacoustic (middle), and US/PA (bottom) images of the tissue mimicking phantom with inclusions containing melanoma cells at a wavelength of 750 nm. Photoacoustic signals were detected from different concentrations of the melanoma cells in the inclusions, because the melanin in the melanoma cells has a strong optical absorption in this laser wavelength. Furthermore, the quantitative analysis of the photoacoustic signal amplitudes measured from the inclusions, using a laser fluence of 5.0 mJ/cm^2, is shown in Figure 2b. The results indicate that the amplitude of the photoacoustic signal is propor-

tional to the concentration of the melanoma cells. The results also indicate that with a fluence of 5.0 mJ/cm^2, a photoacoustic signal can be detected for a concentration of melanoma cells as low as 2.5 × 10^3 cells/μL, which corresponds to 2.5 × 10^4 cells in 10 μL. The sensitivity can be improved by increasing the pulsed laser energy under the ANSI safety limit. Therefore, the photoacoustic imaging method can quantify melanoma cell concentrations with greater sensitivity than MRI based cell-tracking methods [3].

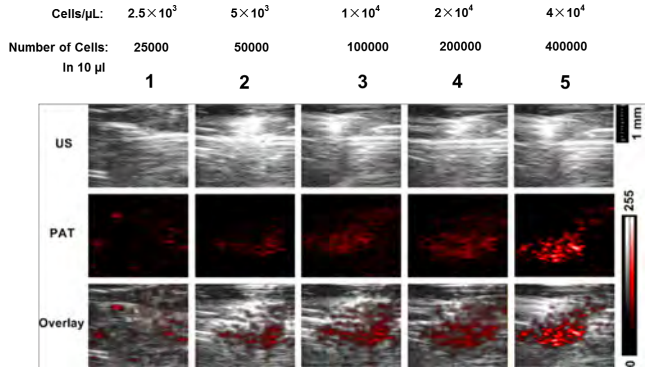

(a)

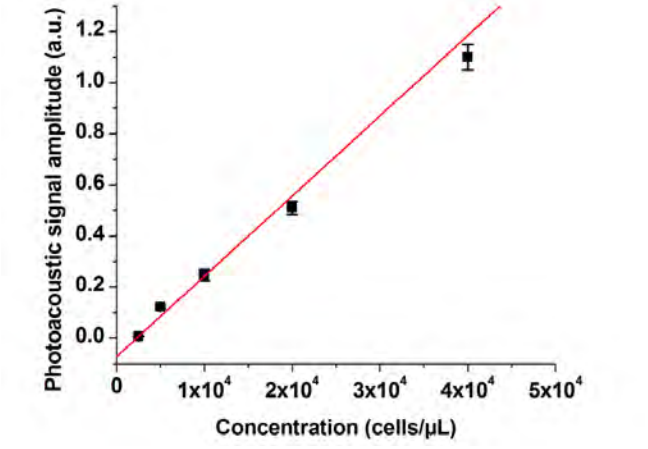

(b)

Fig. 2. Sensitivity of melanoma cells detection with photoacoustic imaging on phantom. (a) Ultrasound (top), photoacoustic (middle), and US/PA images (bottom) of the gelatin phantom with inclusions containing different concentrations of melanoma cells. Photoacoustic images were obtained at a wavelength of 750 nm with a fluence of 5.0 mJ/cm^2. (b) Photoacoustic signal amplitude vs. cell concentration. The graph presents the linear regression fit (with an R2 value of 0.988) of the mean values of the photoacoustic signal amplitude as a function of the cell concentration in a linear scale.

3.2 Imaging penetration depth

To evaluate the imaging penetration depth of photoacoustic imaging for cell tracking, the cell inclusion was imaged at different depths embedded inside a gel phantom from 5 – 13 mm deep. Figure 3 shows the 2-D reconstructed PA (Fig 3a) and US (Fig 3b) image at 810 nm laser wavelength of the melanoma cells in the phantom. These results show that the melanoma cells at the depth of 13 mm inside the phantom can be easily resolved. The image depth can be increased by using a low frequency transducer (13 – 24 MHz) up to 30 mm.

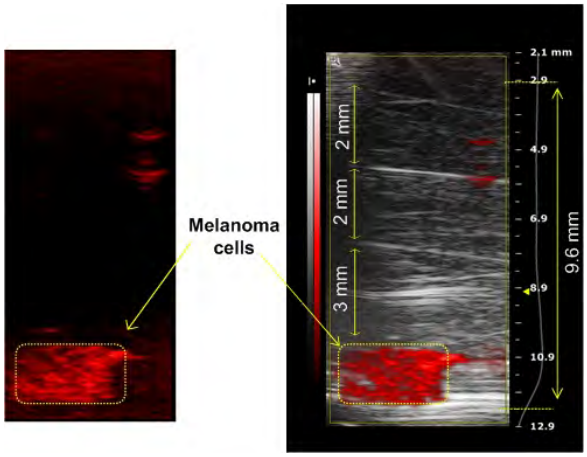

(a) (b)

Fig. 3. Imaging penetration depth of photoacoustic imaging for cell tracking. (a) Photoacoustic, and (b) PA/US images of the gelatin phantom with inclusions containing melanoma cells. The image depth is around 15 mm by high frequency transducer (32 – 55 MHz).

3.3 Tracking melanoma cells in real-time

Figure 4 demonstrates the real-time cell-tracking ability of the PA/US imaging system in flowing melanoma cells. A pump (CZ-74901-15, Cole Parmer Vernon Hills, IL, USA) and a 1 mL standard syringe connected with the plastic tube were used to produce a constant melanoma cell flow in the plastic tube. Laser irradiation of the area in the tube generates the PA signals, which can be detected with an ultrasound array transducer attached to the tube. The tube was imbedded in a tissue mimic phantom; both the phantom and the ultrasound transducer array were immersed in a water containerS. In particular, high speed imaging allows real-time visualization of the moving cells as shown in the images obtained at different time points. Video 1 shows photoacoustic cell-tracking in real time. This exper-

iment demonstrates that PAM has the potential to track melanoma metastatic cells in real time.

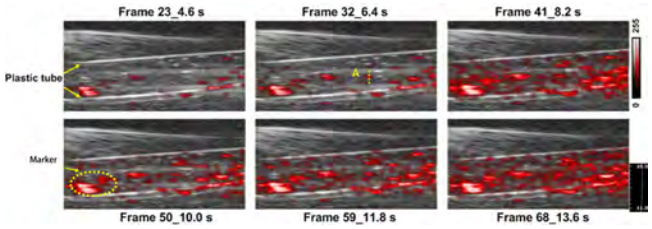

(video)

Fig. 4. Real-time tracking melanoma cells with photoacoustic imaging. (video). The image speed can up to 5 frames/s.

4 Discussion

In summary, we developed a noninvasive cell-tracking method with a label-free photoacoustic imaging technique. The PAM is demonstrated to be sensitive for monitoring very low numbers ($\times 10^4$) of melanoma cells without labeling. Moreover, by using a high-frequency ultrasound array transducer, we can visualize cells in real time with very high resolution. Photoacoustic imaging provides a new method for cancer screening and may offer insight into the underlying biological processes involved in cell therapy including cell survival, migration, homing, engraftment, differentiation, and functions.

The unique advantage of photoacoustic cell-tracking is the possibility of detecting cells without labeling by using the high photoacoustic contrast of pigmented melanoma cells above the background signal of blood [19, 20]. Since photoacoustic methods can provide information on nonfluorescent cellular absorption associated with intrinsic chromophores and pigments, this method can be extended to track any of the molecules inside the body with a specific wavelength in the range of their strong optical absorption (e.g., cytochromes, hemoglobin, carotenoids, melanin, DNA/RNA, water, or lipids). Therefore, cellular PAM may pave the way for many investigators and clinicians to obtain a more in-depth view of the underlying bio-dynamics of cellular treatment modalities. Better, faster, and higher-resolution PAM is on the horizon, and they will play an important role in cell tracking, gene expression, and tumor biology. The advances made in just the past few years have been remarkable, and there is no doubt that continued efforts will result in innovative imaging technologies for both animals and humans. We believe that PAM will accelerate the application of cell therapy in both preclinical and clinical studies.

Acknowledgement: The authors gratefully acknowledge the Department of Defense Prostate Cancer Research Programs W81XWH-13-1-0481 (LX), the National Institutes of Health 1R01 CA133474 and 1R21 A153587, and SRFDP (20124407120012) for funding.

Competing financial interests

The authors declare no competing financial interests.

References

[1] Kircher, M.F., Gambhir, S.S. & Grimm, J. Noninvasive cell-tracking methods. *Nature reviews. Clinical oncology* **8**, 677-688 (2011).
[2] Galanzha, E.I. & Zharov, V.P. Circulating Tumor Cell Detection and Capture by Photoacoustic Flow Cytometry in Vivo and ex Vivo. *Cancers* **5**, 1691-1738 (2013).
[3] de Vries, I.J. et al. Magnetic resonance tracking of dendritic cells in melanoma patients for monitoring of cellular therapy. *Nature biotechnology* **23**, 1407-1413 (2005).
[4] Massoud, T.F. & Gambhir, S.S. Molecular imaging in living subjects: seeing fundamental biological processes in a new light. *Genes & development* **17**, 545-580 (2003).
[5] Freudiger, C.W. et al. Label-free biomedical imaging with high sensitivity by stimulated Raman scattering microscopy. *Science* **322**, 1857-1861 (2008).
[6] Lao, Y., Xing, D., Yang, S. & Xiang, L. Noninvasive photoacoustic imaging of the developing vasculature during early tumor growth. *Physics in medicine and biology* **53**, 4203-4212 (2008).
[7] Xiang, L., Wang, B., Ji, L. & Jiang, H. 4-D photoacoustic tomography. *Scientific reports* **3**, 1113 (2013).
[8] Zhang, H.F., Maslov, K., Stoica, G. & Wang, L.V. Functional photoacoustic microscopy for high-resolution and noninvasive in vivo imaging. *Nature biotechnology* **24**, 848-851 (2006).
[9] Xi, L., Duan, C., Xie, H. & Jiang, H. Miniature probe combining optical-resolution photoacoustic microscopy and optical coherence tomography for in vivo microcirculation study. *Applied optics* **52**, 1928-1931 (2013).
[10] Zhang, C., Cheng, Y.J., Chen, J., Wickline, S. & Wang, L.V. Label-free photoacoustic microscopy of myocardial sheet architecture. *Journal of biomedical optics* **17**, 060506 (2012).
[11] Zhou, Y., Zhang, C., Yao, D.K. & Wang, L.V. Photoacoustic microscopy of bilirubin in tissue phantoms. *Journal of biomedical optics* **17**, 126019 (2012).
[12] Yao, D.K., Maslov, K., Shung, K.K., Zhou, Q. & Wang, L.V. In vivo label-free photoacoustic microscopy of cell nuclei by excitation of DNA and RNA. *Optics letters* **35**, 4139-4141 (2010).
[13] Xu, Z., Zhu, Q. & Wang, L.V. In vivo photoacoustic tomography of mouse cerebral edema induced by cold injury. *Journal of*

biomedical optics **16**, 066020 (2011).
[14] Wang, H.W. et al. Label-free bond-selective imaging by listening to vibrationally excited molecules. *Physical review letters* **106**, 238106 (2011).
[15] Zhang, C., Zhang, Y.S., Yao, D.K., Xia, Y. & Wang, L.V. Label-free photoacoustic microscopy of cytochromes. *Journal of biomedical optics* **18**, 20504 (2013).
[16] Zhang, H.F., Maslov, K. & Wang, L.V. In vivo imaging of subcutaneous structures using functional photoacoustic microscopy. *Nature protocols* **2**, 797-804 (2007).
[17] Talukdar, Y., Avti, P.K., Sun, J. & Sitharaman, B. Multimodal Ultrasound-Photoacoustic Imaging of Tissue Engineering Scaffolds and Blood Oxygen Saturation In and Around the Scaffolds. *Tissue engineering. Part C, Methods* (2013).
[18] Jiang, H. & Xu, Y. Phase-contrast imaging of tissue using near-infrared diffusing light. *Medical physics* **30**, 1048-1051 (2003).
[19] Nedosekin, D.A., Sarimollaoglu, M., Ye, J.H., Galanzha, E.I. & Zharov, V.P. In vivo ultra-fast photoacoustic flow cytometry of circulating human melanoma cells using near-infrared high-pulse rate lasers. *Cytometry. Part A : the journal of the International Society for Analytical Cytology* **79**, 825-833 (2011).
[20] Weight, R.M., Viator, J.A., Dale, P.S., Caldwell, C.W. & Lisle, A.E. Photoacoustic detection of metastatic melanoma cells in the human circulatory system. *Optics letters* **31**, 2998-3000 (2006).